Technion - Israel Institute of Technology

Robust Guidance and Control (038781)

Spring 2018

Project 1 - Linear Guidance

Prof. Shaul Gutman

Submitted by : Daniel Engelsman

July 17, 2018

Contents

List of Figures

Introduction

Given a TVC (Thrust Vectoring Control) interception system, where most of the missile environment is in higher atmosphere, steering is performed exclusively by the nozzle deflection (ϕ) controlling the desired angle (θ).

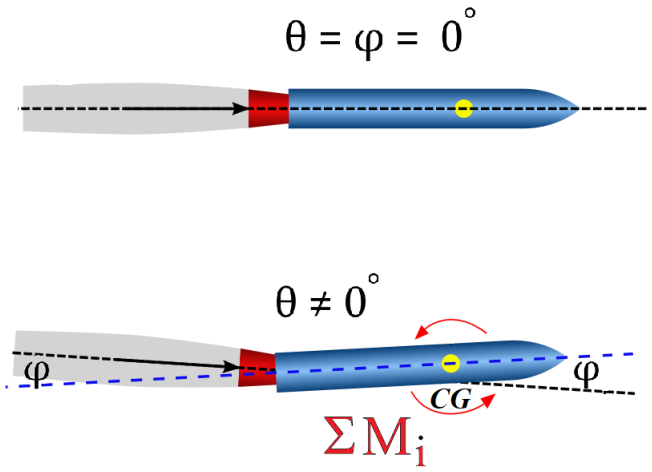

Figure 1: Simple analysis of the dynamic model

There are 2 admissible configurations to satisfy missile's steering :
(i) Front Steering - jet nozzle is in the **Front**. ϕ is obtained in the θ direction.
(ii) Rear Steering - jet nozzle is in the **Rear**. ϕ is obtained **opposited** to desired θ direction.

In this project we will analyze the dynamic response (inner $G_M(s)$) of the autopilot on the guidance control (outer loop), and see back and forth how one's design influences the other.

Assumptions Made

- α - Angle of attack, and δ - Servo deflection, are approximated as small angles.
- Longitudinal velocity (V_M) is constant, allowing us discussing only latteral manuevers.
- The missile's center of pressure **coincides** with the center of gravity. The missile's motion is given by **thrust**, and **lift** uses only for manuevering.
- No aerodynamic Effects - In order to keep the problem at a reasonable order (n ≤ 3), one must ignore extreme atmospheric effects upon the missile. Hence, $\alpha \approx 0$ all along analysis process. It is of course similar to missiles in outer space, where only rigid body dynamics govern. Therefore, Angle Of Attack (α) can be neglected and we get $\theta = \cancelto{0}{\alpha} + \gamma$, where θ is w.r.t inertial horizon, and γ is the body angle.
- $\theta \leq 90$ to ensure one constant reference frame along analysis.
- $\dot{r}_{cg} = 0$: Center of gravity location remains constant, despite using solid propellant.
- **Guidance** is implemented after 1st order **linearization** of the **kinematics**.

List of Abbreviations

AP	Autopilot
MD	Miss Distance
MP	Minimum Phase
NMP	Non Minimum Phase
PN	Proportional Navigation
SR	Step Response
Vc	Closing Speed
ZEM	Zero Effort Miss

1 Classic Controller Design

Note: In this project we get a high degree of freedom to design the system "due to our understanding". On my opinion, we're facing an optimization problem with 2 constraints. The first guideline is demanding a reasonable rise time relatively to the servo's time constant ($t_r \leq 10\tau$), While the second is getting the best stability margins in that frame. Here :

$$G_M(s) = \frac{Ks^2 + KM_\delta}{\tau s^3 + (1+K)s^2 + k_{\dot{\gamma}} M_\delta s + KM_\delta}$$

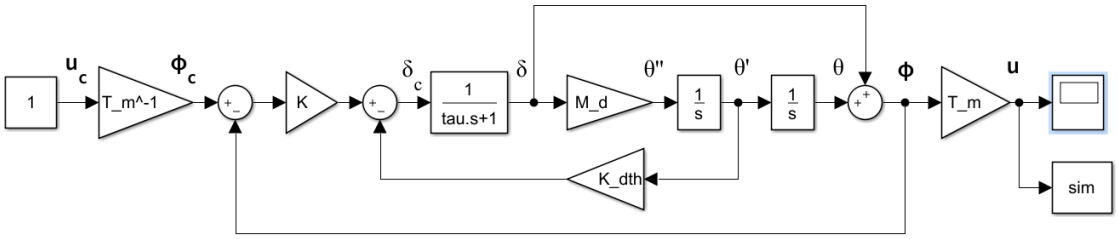

Figure 2: The Auto-Pilot dynamics and its correlated $G_M(s)$

Since no initial "solid" constraint is given as for the dynamic response, we will perform trial and error method of the optimization problem, until reaching satisfactory.

Firstly, running the step response code that spans the "K" values under an initial guessed $K_{\dot{\theta}}$. **Note**: The positive side (**K>0**) of the 3D plot belongs to the MP configuration and corresponds to a $+K_{\dot{\theta}}$, while the left side (**K<0**) is of the NMP and has $-K_{\dot{\theta}}$. In the following pages I will perform manual optimization, showing the long way towards robust values.

1.1 Controller Design - Sensitivity Tests

Let us assume a mesh grid comprised of the discussed $G_M(s)$'s step responses (SR), over the K-Time plane, where $K_{\dot{\theta}}$ is constant :

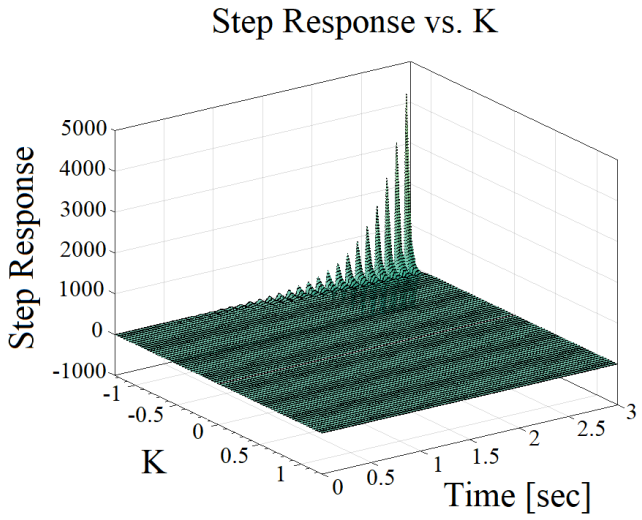

Figure 3: Step Response Matrix for $K_{\dot{\theta}} = \pm 1$

It is clear that we get a flat SR matrix with rapid divergence at the top right corner (Thousands % deviation), whereas K < 0. We shall therefore, narrow K range in half.

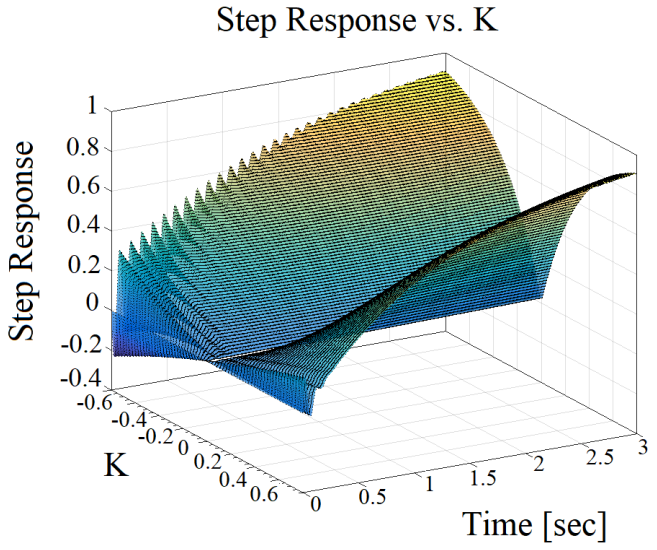

Figure 4: Step Response Matrix for $K_{\dot{\theta}} = \pm 1$

Definitely useful, as we can now see a more familiar formation of SR rising towards "1" value. However, each side reacts differently where the negative (**NMP**) exhibits unstable SR with spikes, whereas the positive (**MP**) shows a smoother family of SR.

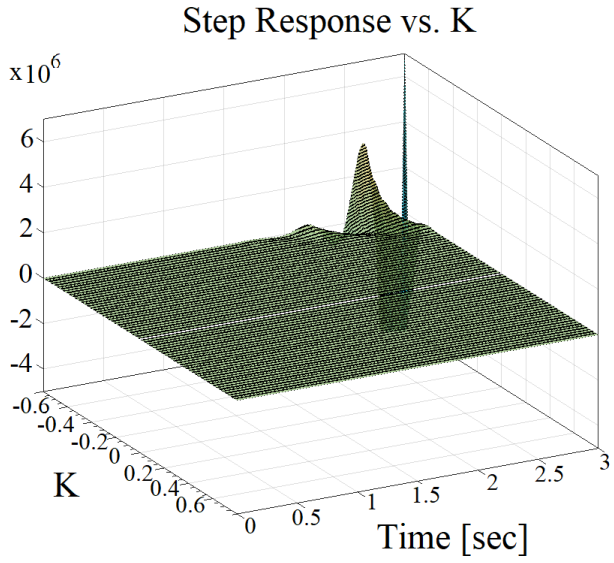

Figure 5: Step response of AP inner loop Vs. $K_{\dot{\theta}} = \pm 0.01$

This time I minimized $K_{\dot{\theta}}$ in order to check the SR matrix. As can be seen, we once again get a huge unstable "Explosion" at the margins. Therefore, I'll aim for a "middle" K value and shorten the time axis towards the desired time frame ($t_r = 10\tau$).

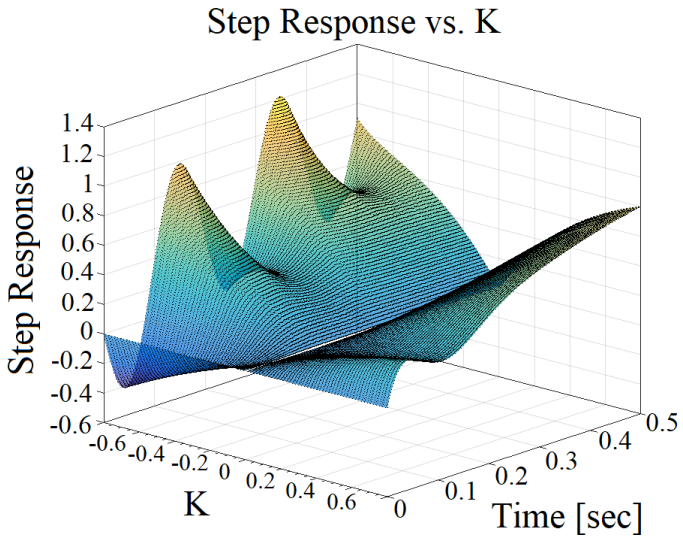

Figure 6: Step response of AP inner loop Vs. $K_{\dot{\theta}} = \pm 0.1$

This time we can see reasonable domain where both **MP** and **NMP** are getting towards "1" in almost 90 % of the t_r. However, the **NMP** still exhibits unstable behaviour that's characterized by undesired fluctuations. Let us reduce once again $K_{\dot{\theta}}$ values :

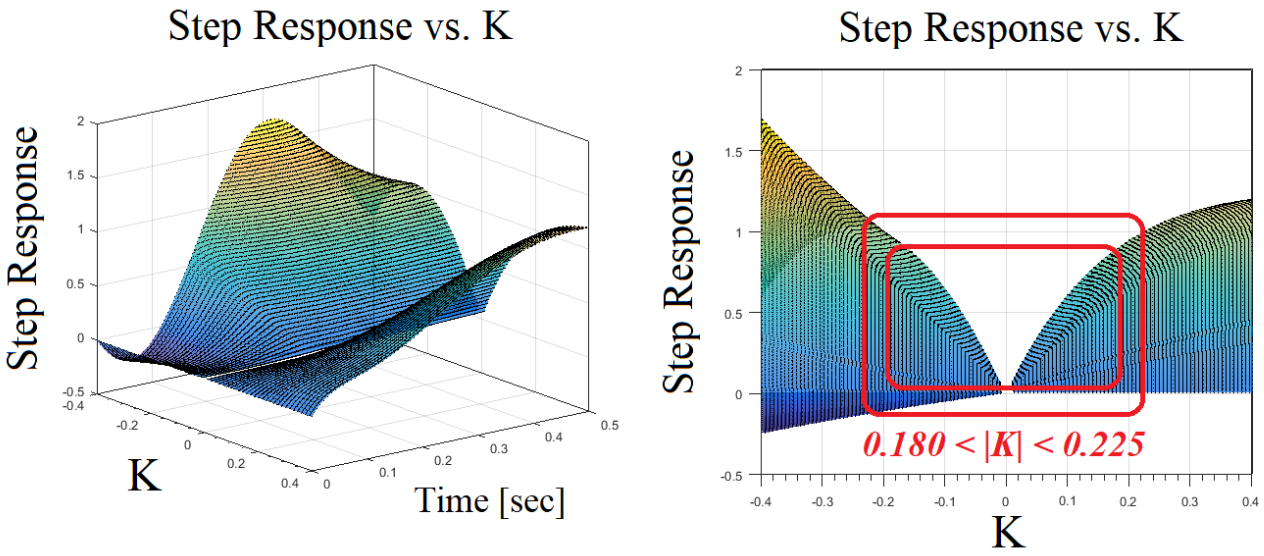

Figure 7: Step response of AP inner loop Vs. $K_{\dot{\theta}} = \pm 0.05$

Finally we arrived at the desired K domain that satisfies the requirement of $(t_r = 10 \cdot \tau)$. **Note** that the NMP performs **Inverse Response** at the beginning of the SR, as opposed to the MP that rises directly. More traditionally, we can present these sets of SR as :

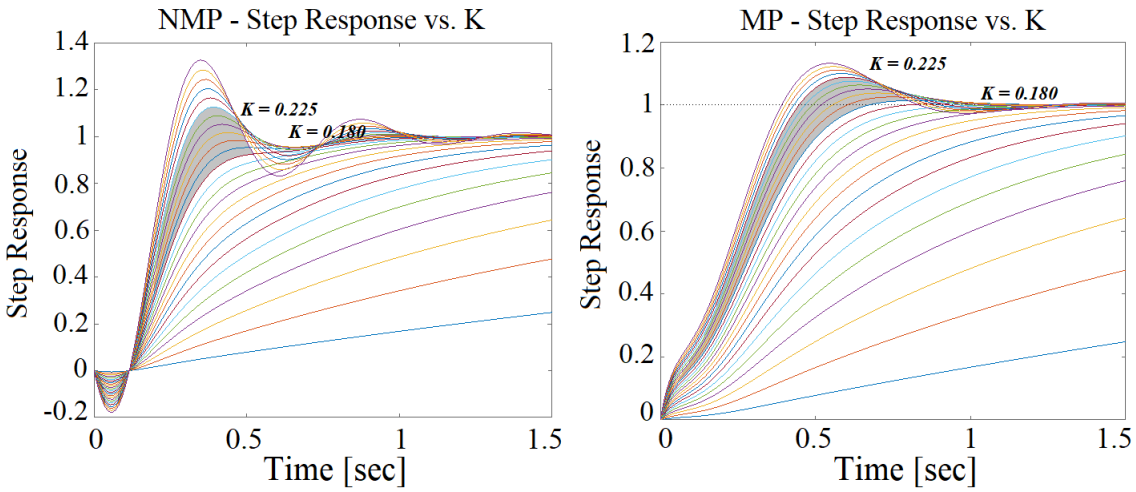

Figure 8: Cross Sectioning of SR for $0.180 < |K| < 0.225$

To conclude, I chose the following "rounded" values to work with :

$$K_{\dot{\theta}} = \pm 0.05 \quad ; \quad K = \pm 0.2.$$

MP - Positive values, and **NMP** - Negative values. Mind that a symmetry conditions exist in the reference frame I denoted (**Fig.** 7) between the 2 configurations.

2 Navigation Performance Vs. Bounded Target Manuever

As seen on class, we will use the "adjoint" algorithm. One of its properties is the inversion of forward time into reverse time, hereby denoted as t_{go}. In order to obtain feasible values, we must plug some "real" numbers into the scenario : $V_c = 1250\frac{m}{sec^2}$, $\rho_w = 10^{-4}$, $\Phi_{11}(0) = 1$.

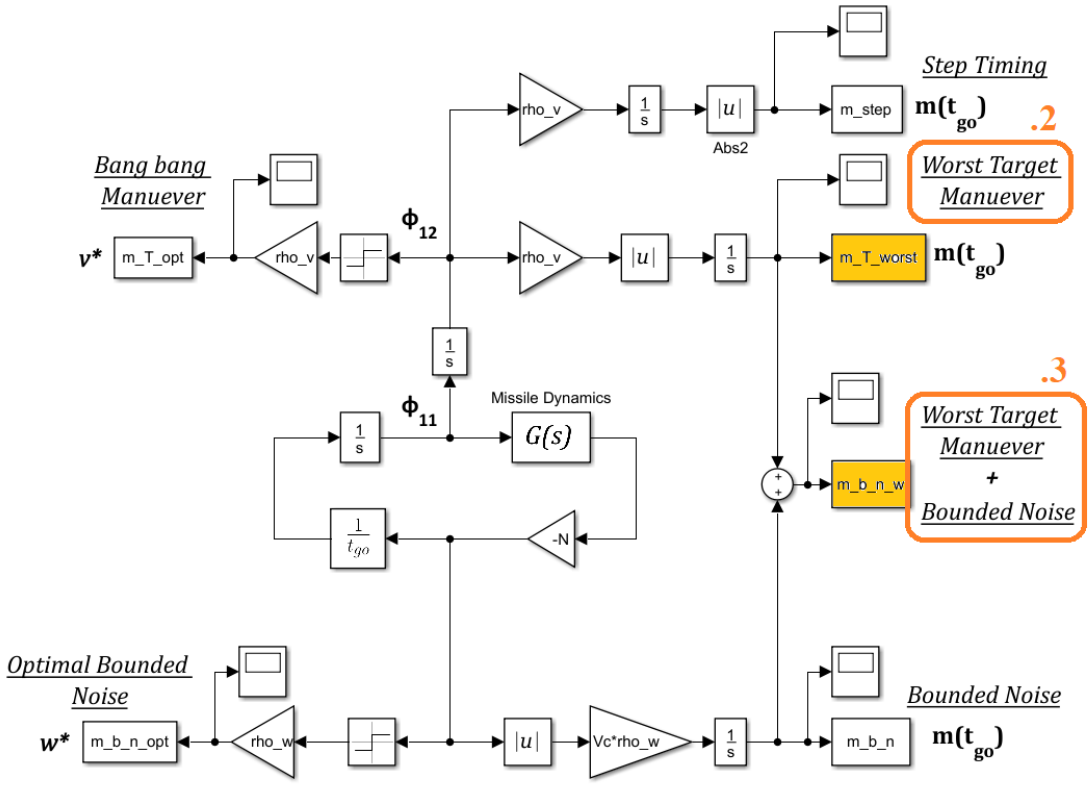

Figure 9: Full Adjoint Algorithm of the system

2.1 Bounded Target Manuever - Simulation

Here we'll examine the miss distance (**MD**) performances under a set of bounded target manuevers. From left is a 3D plot of MD Vs. t_{go}, in a growing ρ_v's, and from right is a side cross-section. The **lower** MD is pertained to the **MP**, and the **upper** to the **NMP**.

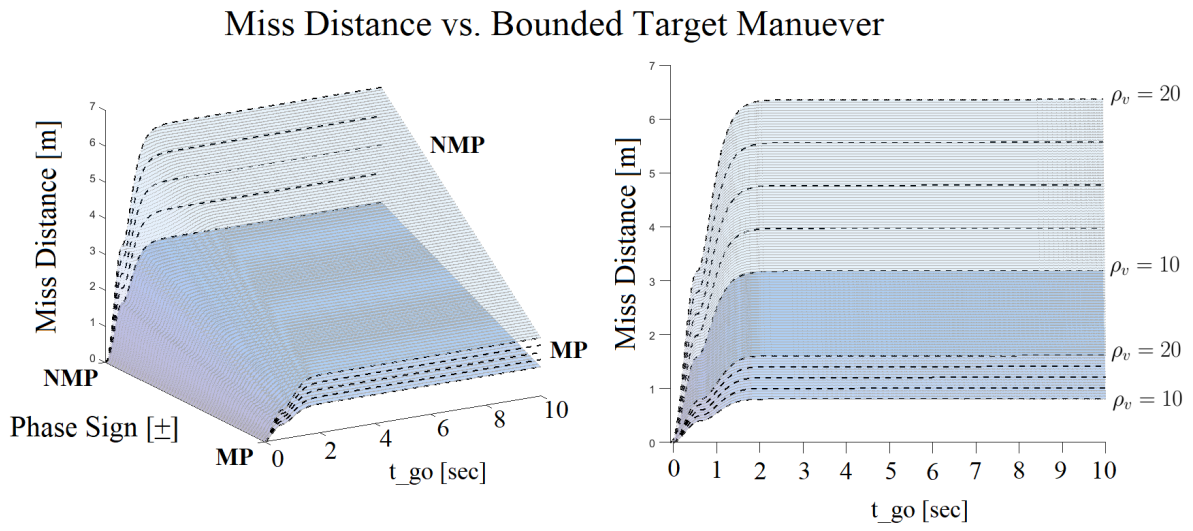

Figure 10: Miss distance Vs. Bounded target manuever

For the sake of simplicity let us narrow the t_{go} axis range towards the origin :

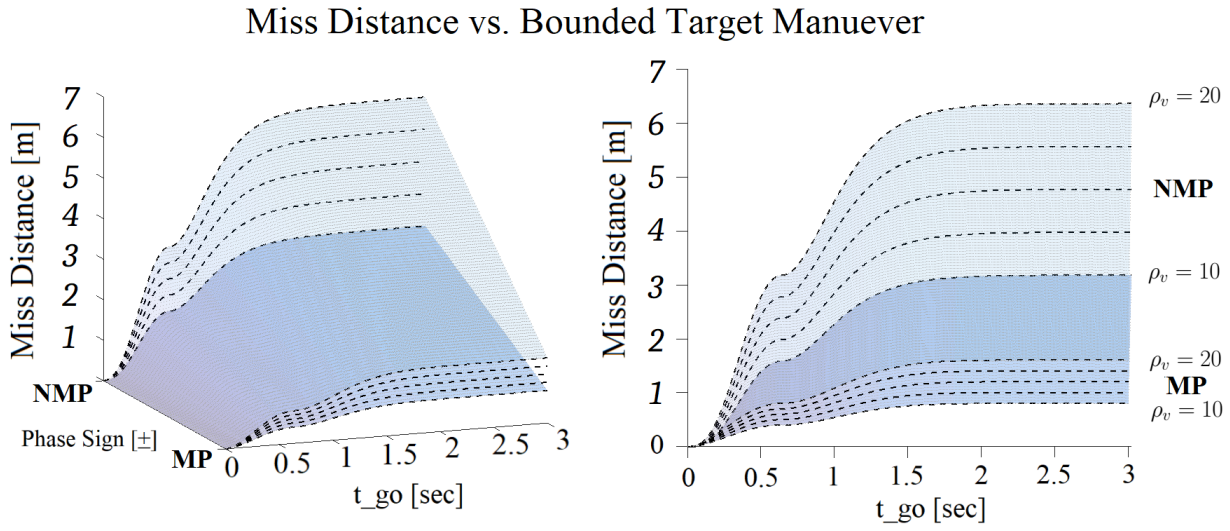

Figure 11: Miss distance Vs. Bounded target manuever

2.2 Bounded Target Manuever - Discussion

Despite major differences between both cases, there are few similarities that worth discussion:
(i) **MP** configuration achieves better MD, about 4 times smaller than that of **NMP**.
(ii) Rising time is equal at both configurations, since it's relies on the same dynamics $G_M(s)$.
(iii) The MD stays constant along t_{go} until reaching a critical t_{cr} value, from which the MD drops significantly towards ZMD (MD $\rightarrow$ 0).

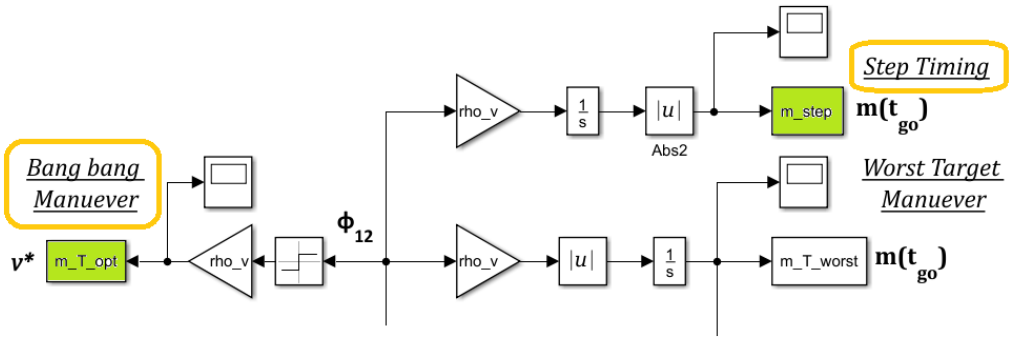

Figure 12: optimal target manuever and step timing scopes

However, an important question that arise is : What is the meaning of these local **"shoulders"** on $t_{go} = 0.66$ [sec] ? Let's look in the denoted scopes (**Fig.** 12) and correlate :

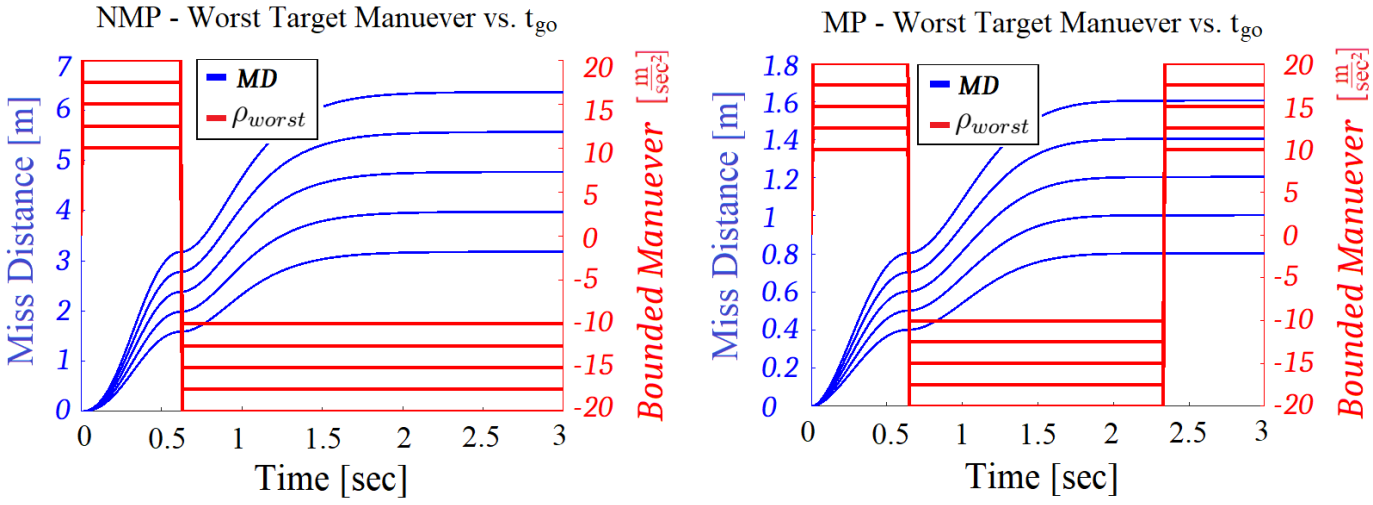

Figure 13: MD Vs. Worst Target Manuever

As shown, these shoulders correlate with the MD just when the target breaks ρ_v direction. Here at $t_{go} = 0.66$ [sec], it performs **optimal** Manuever - AKA **"Bang bang Manuever"**. One can see that the canard configuration has one **more** additional manuevering timing, while the tail is forced to conduct it, only moment before t_f. That "extra" manuever is translated to the better MD the canard achieves.

3 Performance Vs Bounded Manuever & Noise

Here we're requested to examine MD when the Target experiences both bounded manuever and noise. In front of the dynamics block I've used compatible noise filter $\left[\frac{1}{0.01s+1}\right]$. Luckily, the problem "lives" in a **Linear World** where super-position combination can be made. Therefore, we'd start off simulating for both configurations, a set of bounded noises **isolated**, since target **does not accelerate** ($\rho_v = 0$).

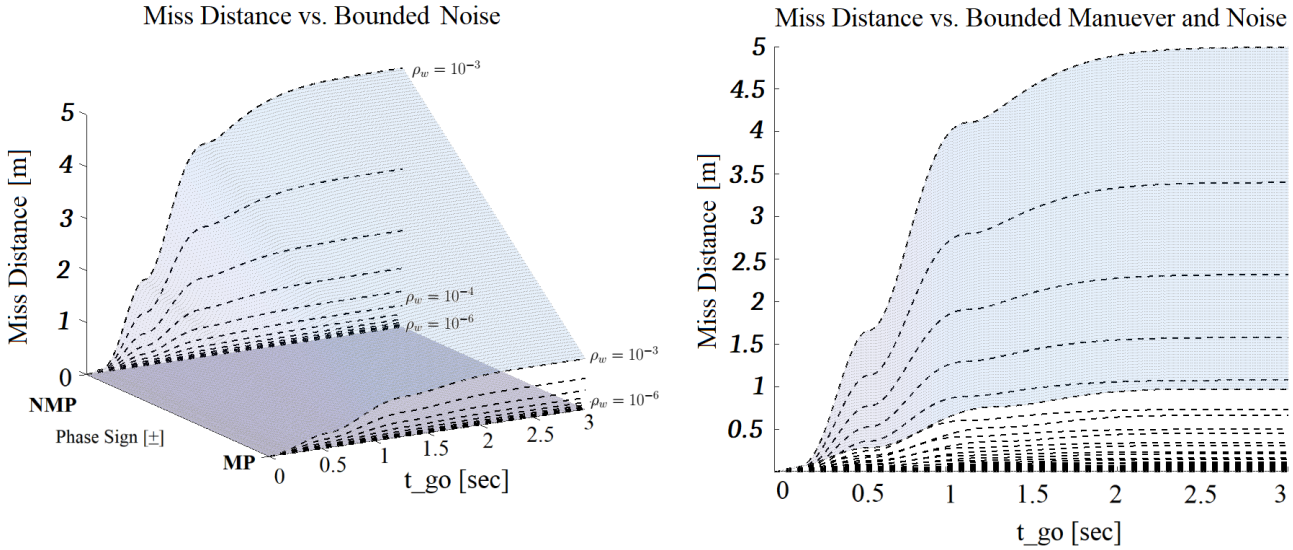

Figure 14: Miss distance Vs. Bounded Noise ($\rho_v = 0$)

And now we'll run a set of bounded noises, when the target **does accelerate** ($\rho_v = 15$):

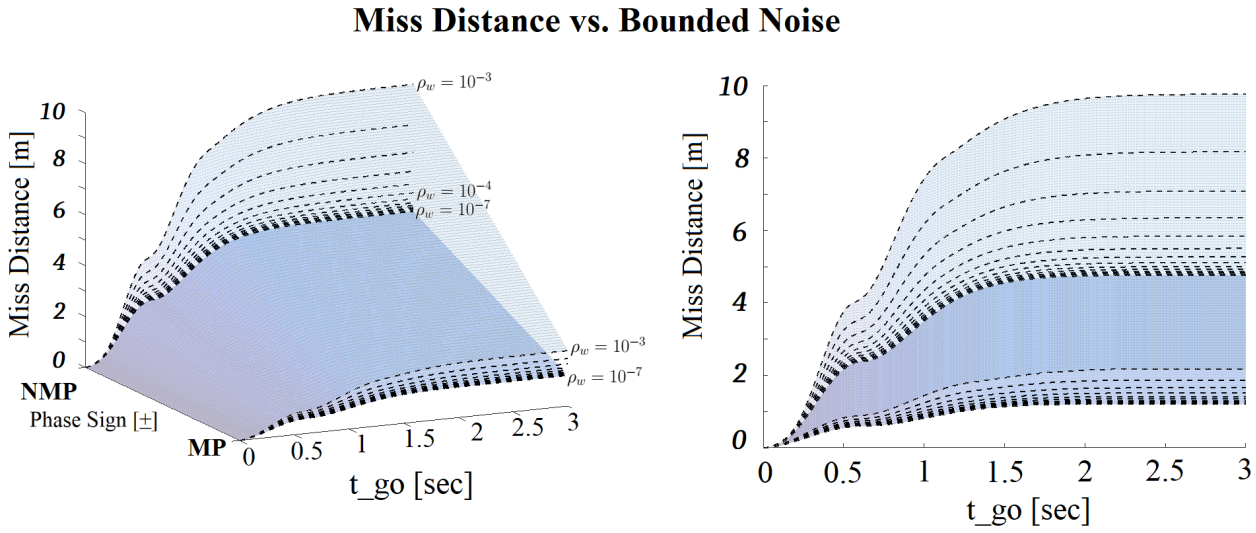

Figure 15: Settled Miss distance Vs. Bounded Noise ($\rho_v = 15$)

As mentioned above, the linearity of the problem take place, and MD being simply summed.

3.1 Bounded Target Manuever & Noise - Discussion

There are few points worth noticing after the mentioned analysis :

(i) Both configurations form a thick **black base** when ρ_w is small. That is to say that noise takes action only from a certain value, and before all MD's are equal.

(ii) When noise is $\rho_w \geq 10^{-4}$, results start "exploding" and MDs become useless (**Fig.** 16).

(iii) *Like* in the previous chapter, we can see **"shoulders"** when MD drops down. However *Unlike* previously, they last longer. But what does it mean? To ensure interception, the missile needs now **longer (3X)** manuevering duration than previously. The target however, enjoys **wider** time span, and might escape from warhead's damage zone, and survive. Therefore, ρ_v noises are **weakening** the missile supremacy over the Target.

Let us now look at the miss distance vs. the noise magnitude, in a semi-log x graph :

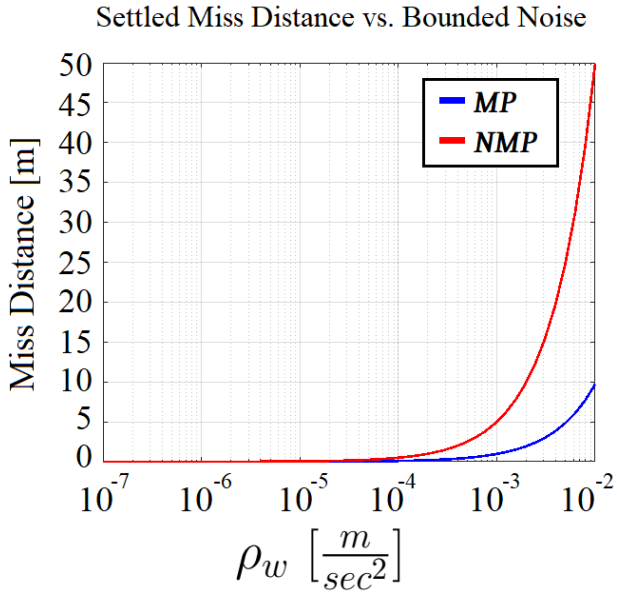

Figure 16: Settled Miss distance Vs. Bounded Noise ($\rho_v = 0$)

We can see the differences between each configuration's result. The next graph is the MD extents at both configurations when bounded noise is added to the scenario :

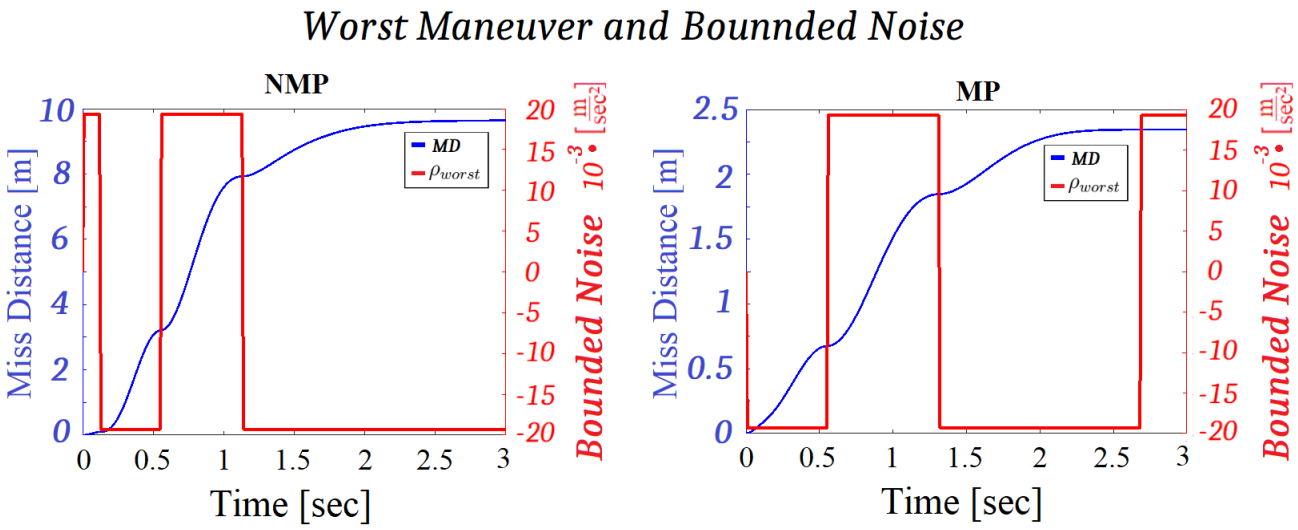

Figure 17: MD vs. Worst Maneuver and Bounded noise ($\rho_v = 15$, $\rho_w = \pm 20 \cdot 10^{-3}$)

4 System's sensitivity to different parameters

In this section we'll examine the PN sensitivity to a change in the initial parameters, where the default conditions are $\rho_v = 15[\frac{m}{s^2}]$ and $\rho_w = 10^{-4}[\frac{m}{s^2}]$. We'll run the simulations under set of values each time, and check the scopes for suspicious reactions.

Analysis of Parameters

Symbol	Parameter	Analysis Span	Units
M_δ	Stability Derivative	[10 1,000]	$[\frac{1}{s^2}]$
τ	Time Constant	[0.001, 1]	$[s]$
V_c	Closing Speed	[100, 10,000]	$[\frac{m}{s}]$
$\frac{T}{m}$	Longitudinal Acceleration	[50, 500]	$[\frac{m}{s^2}]$
N	Navigation Constant	[2, 10]	[-]

Notes :

1: Both (ρ_v,ρ_w) are constants and **only** MD of target's **worst** manuever will be presented.

2: Amidst the "ocean of results", I'll present **only** the **significant** ones, for sake of clarity.

3: In each of the following graphs, the Z axis presents the subjected response, while the Y axis scales from negative (**NMP**) to positive gain (**MP**) respectively.

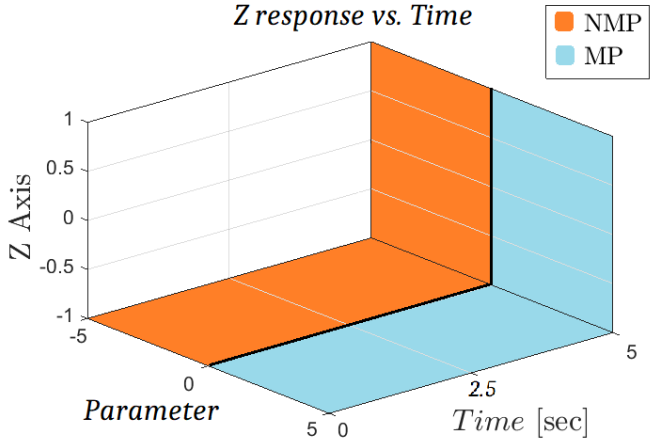

Figure 18: Bisection of 3D space into 2 configurations

4.1 Sensitivity to M_δ

The main variable in this section is the Miss Distance Vs. the M_δ magnitude.
Accelerations are constant and bounded along simulations ($\rho_v = 15[\frac{m}{s^2}]$ and $\rho_w = 10^{-4}[\frac{m}{s^2}]$).

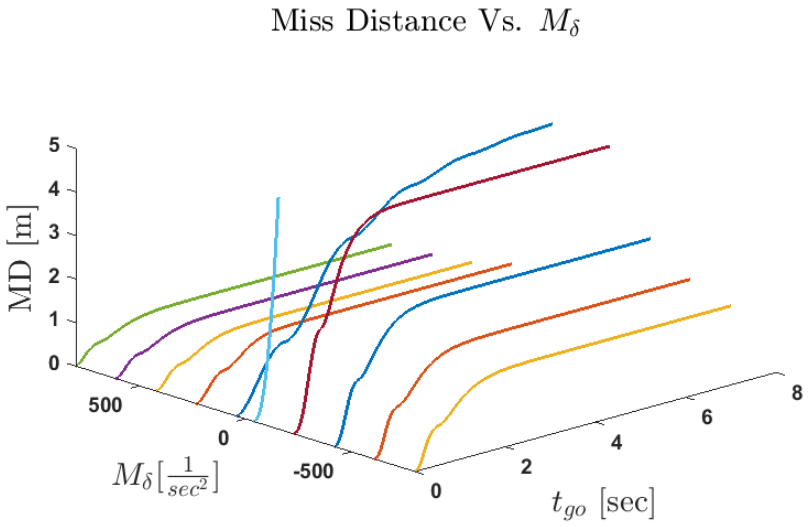

Figure 19: Miss Distance Vs. M_d

Around $|M_d| \leq 100$ the MD **diverges quickly** at both configurations. However, the NMP is much **vulnerable** to the change as it requires stronger MD values to achieve zero MD. But **when** exactly along flight time, the maneuver and bounded noise take action ?

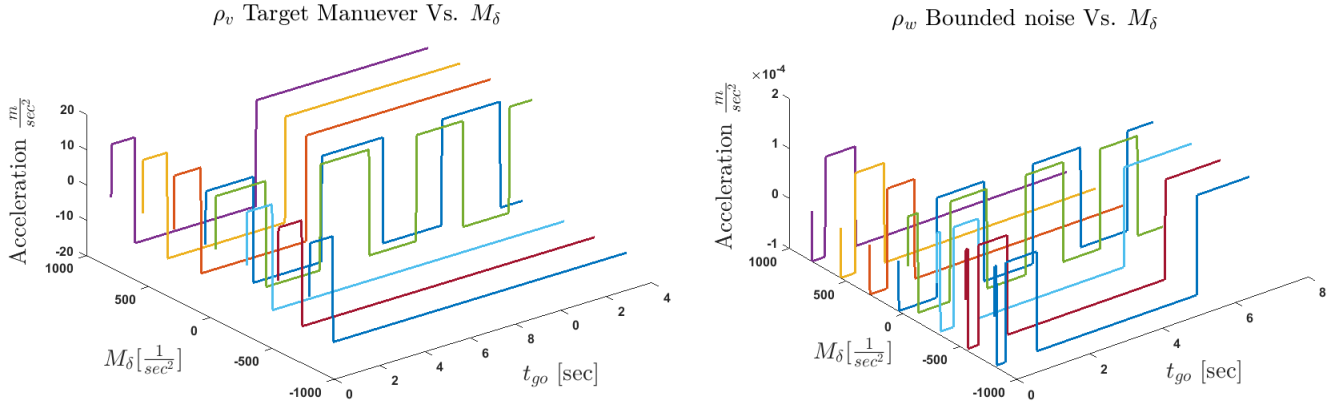

Figure 20: Bounded ρ_v and ρ_w Vs. M_d

Much like the figure above, when $|M_d| \leq 100$ the interceptor coerce tough manuevers on the target in order to escape. Both accelerations (ρ_v and ρ_w) exhibit frequent changes in sign boundary in order to achieve **optimal** manuever. But when $|M_d|$ value increases, the changes **decay** since escaping the "stronger" missile becomes almost useless. At the $|M_d|$ margins, optimal manuever will be obtained only moments before $t \to t_f$.

4.2 Sensitivity to τ

τ is the reduced order dynamics of the servo unit. The δ output is the element that initiates the pitch moment that eventually being translated into $\ddot{\theta}$. Therefore beforehand, we may expect that the MD performance will correspond directly to duration of τ.

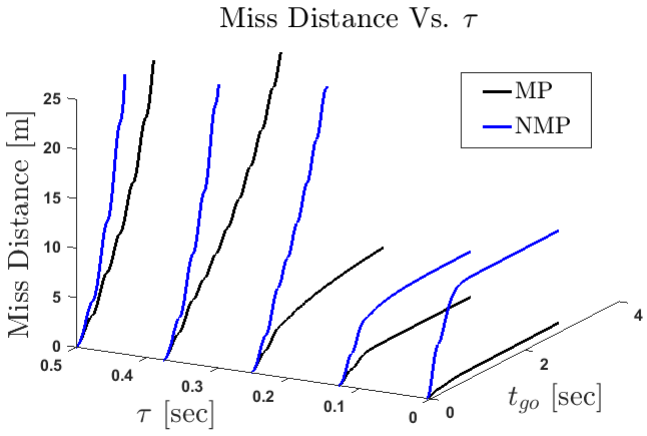

Figure 21: MD Vs. $\tau \in [0.005\ 0.5]$

Once again we see MP's priority over NMP configuration. For any given τ, the MP performance is significantly better, although towards bigger values - both exhibit poor performance resulting in convergence. **Interestingly**, NMP shows anomaly around $\tau = 0.125$ [sec]. Instead of showing consecutive increase in MD, we get **Better MD**, implying that there's an optimal domain where MD can be minimized.

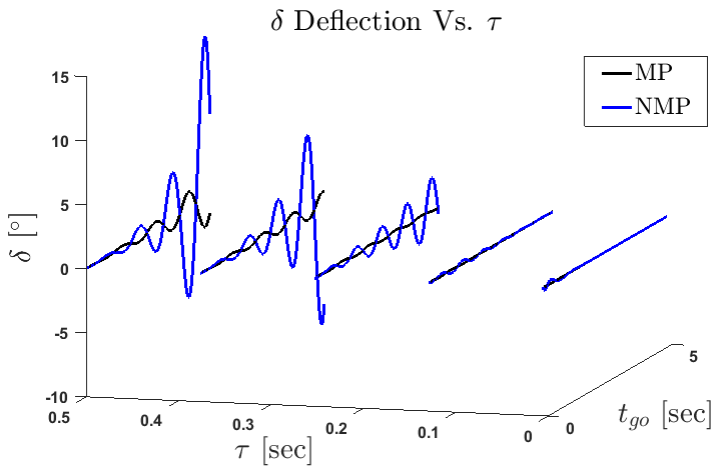

Figure 22: δ Deflection Vs. $\tau \in [0.005\ 0.05]$

τ reflects the servo's mechanical ability to implement the guidance command. When $\tau \sim 0.5$ [sec] both MP and NMP saturates ($\delta \sim 20$ [°]), and **Linearity** assumption decays.

4.3 Sensitivity to V_c

In our adjoint system, the only element that is dependent on V_c is the bounded noise MD (**Fig.** 24). Although when combining bounded noise MD with Worst target manuever MD, it might affect. But very few though, as it is a function of both ρ_w and V_c.

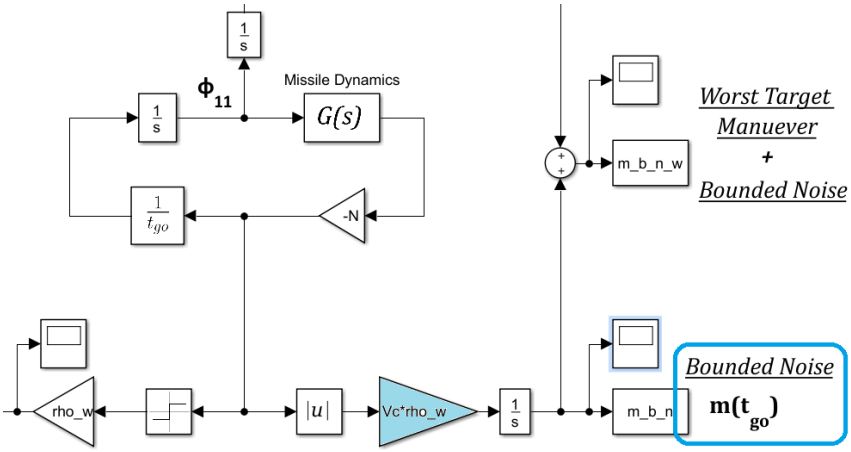

Figure 23: Miss Distance stemmed by bounded noise Vs. V_c

Recalling the magnitudes : $\rho_w = 10^{-4} \quad [\frac{m}{sec^2}]$ and $100 \geq V_c \leq 10000 \quad [\frac{m}{sec}]$. It is therefore not a big surprise that their product yields small MDs, almost normalized to "1".

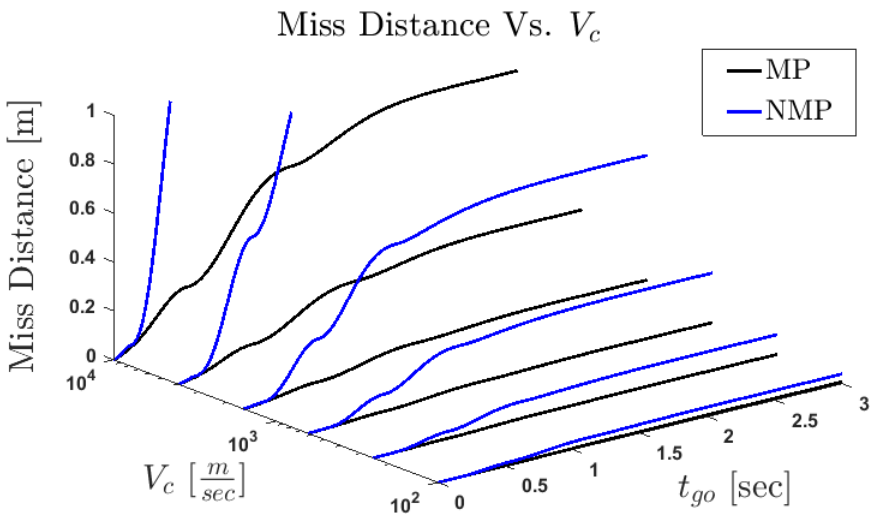

Figure 24: Miss Distance stemmed by bounded noise Vs. V_c

At low speeds, the MD of both configurations is negligible. But when reaching "insanely" high closing speeds ($V_c \sim 10^4 \quad [\frac{m}{sec}]$), the MD starts increasing gradually, whereas the NMP's MD is worse than MP.

4.4 Sensitivity to $\frac{T}{m}$

$\frac{T}{m}$ denotes the interceptor's longitudinal acceleration. Let us run a set up to 50 $g's$ $[\frac{m}{sec^2}]$:

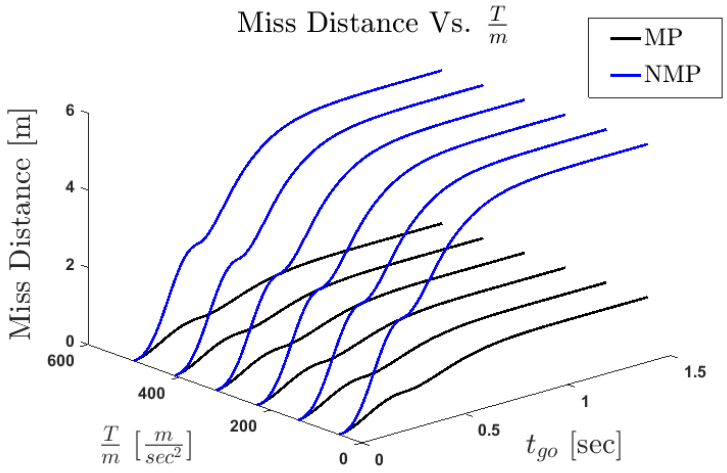

Figure 25: Miss Distance stemmed by bounded noise Vs. V_c

We can see that regardless the magnitude of the acceleration the MD remains unchanged. However let us check the δ deflection to make sure that it is indeed ineffectual.

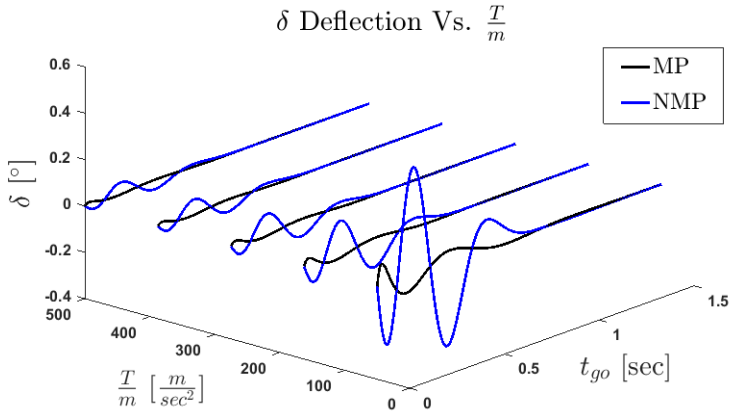

Figure 26: Miss Distance stemmed by bounded noise Vs. V_c

As shown, δ is already small at low values, and keeps decreasing when $\frac{T}{m}$ increases.

4.5 Sensitivity to N'

In proportional navigation, N' denotes the Navigation Constant that ensures MD convergence. in a far off lookout, it seems that MP configuration is almost ineffectual by the N changes, whereas the NMP immediately diverges.

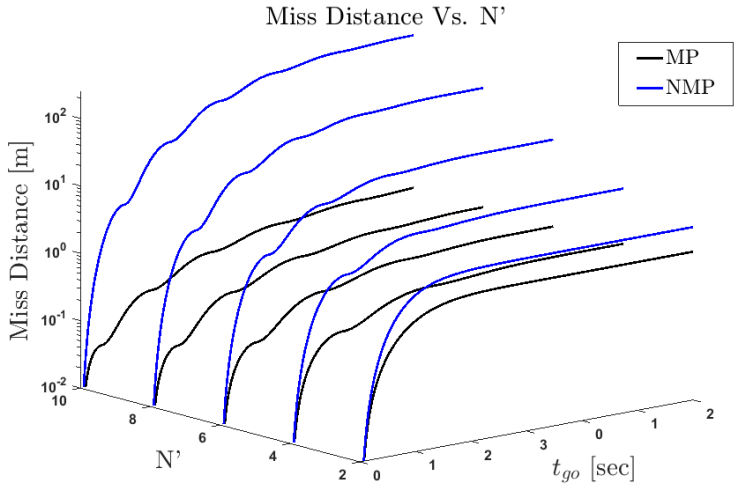

Figure 27: Miss Distance Vs. Navigation Constant $N' \in [2\ 10]$

So who's enjoying the N' navigation constant? Depends on who you are asking.
Looking closely : The MP's MD improves proportionally to N', while NMP worsens :

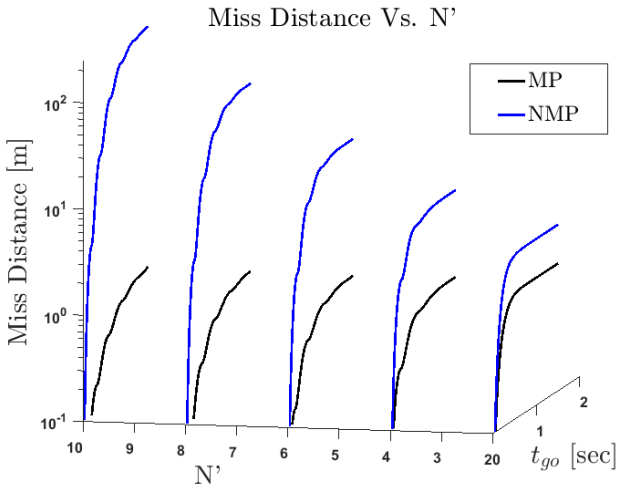

Figure 28: Miss Distance Vs. Navigation Constant $N' \in [2\ 10]$

5 Revision of Feedback's Gains

After examining the influence of each parameter, we will try now to find the best calibration of "K gains", that optimizes the Minimum MD. In **section 2** we've seen the sensitive relationship between inner loop $K_{\dot{\theta}}$ and outer loop K. While K can be "stretched" into wide range of values, $K_{\dot{\theta}}$ is strongly limited. Being optimized at $K_{\dot{\theta}} = 0.05$, we will now re-tune K in attempt to minimize the MD.

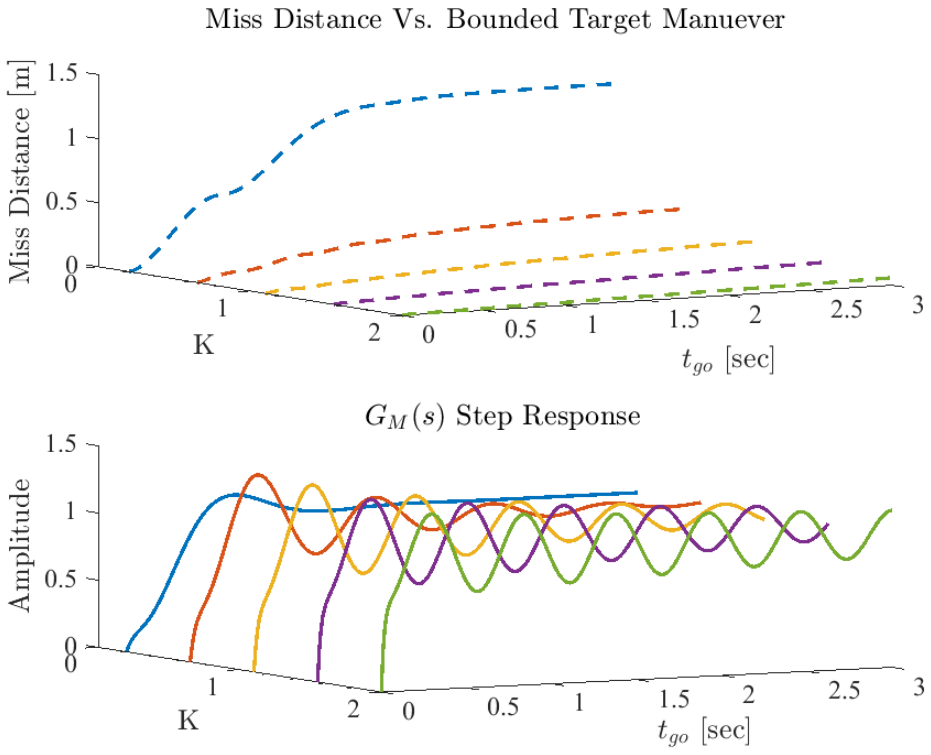

Figure 29: **MP configuration** : MD and SR Vs. $K \in [0.2\ 2]$

First from right (**Blue**) is the **original** simulation from **section 2**, and in the lower subplot is the correspondent SR. Interestingly, the more we increase K values, the less MD goes. Contrarily, the SR **loses damping** and exhibits sinusoidal behaviour. As seen, K is optimized around $2.5 \leq K \geq 3.5$.

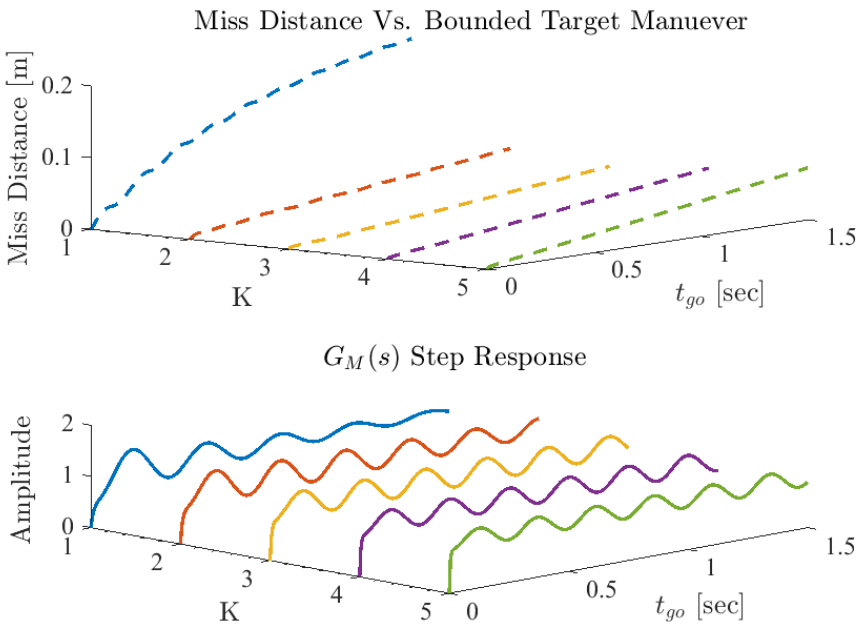

Figure 30: **MP configuration** : MD and SR Vs. $K \in [1\ 5]$

Now we shall check the K re-tuning under the NMP configuration. Originally, I chose $K_{\dot{\theta}}$ and K values which acted symmetrically at both configurations. However, once we step out of that comfort zone, NMP needs to be stabilized with its own gains.

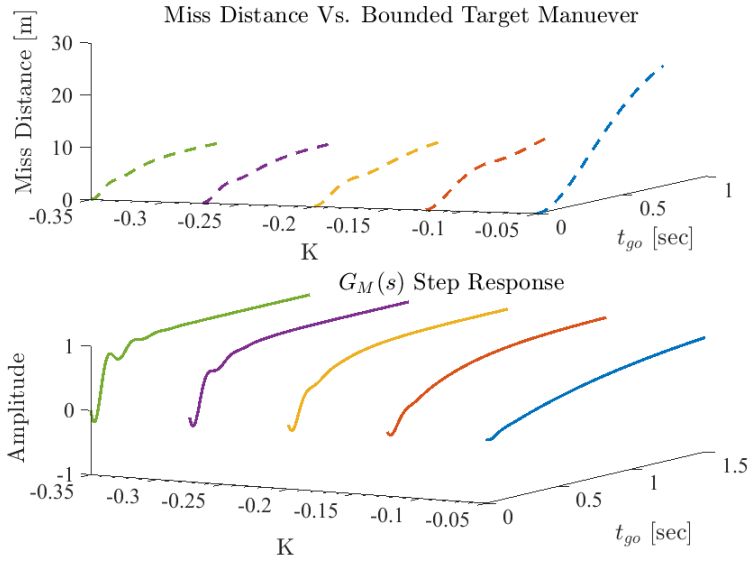

Figure 31: **NMP configuration** : MD and SR Vs. $K \in$ [-0.1 -0.35]

Increasing K gains somewhat more, and **divergence** arises quickly, either at MD or SR analysis. Unlike in the MP configuration, bigger K's lead to system's instability, which is infeasible.

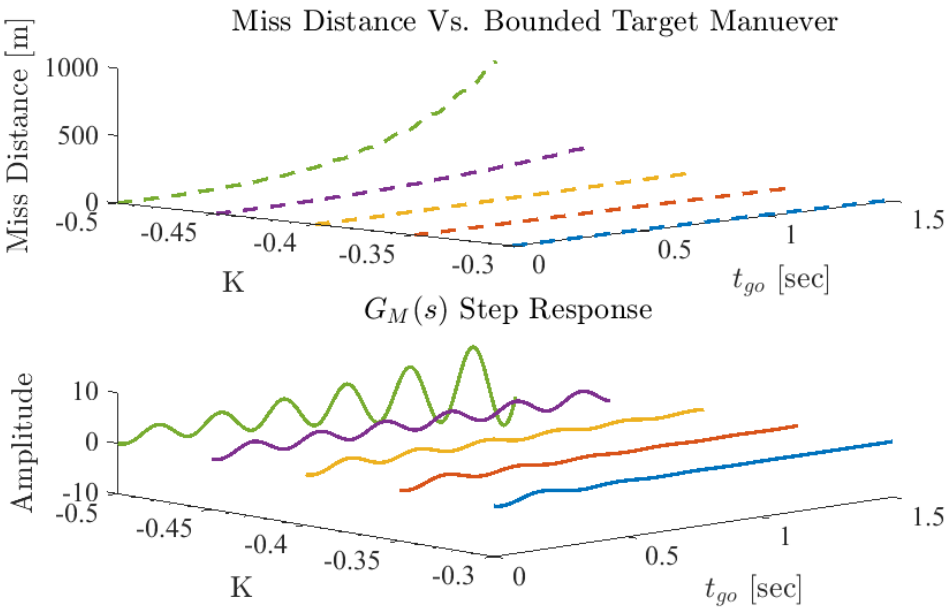

Figure 32: **NMP configuration** : MD and SR Vs. $K \in$ [-0.3 -0.5]

Conclusion : When MD's optimization is the major constraint in front of the designers' eyes, all means are acceptable, even **on account of the** $G_M(s)$ **stability**. However, As seen all along the project, the NMP configuration shows higher sensitivity to changes in gains and parameters.

6 Miss Distance Vs. Servo's Saturation

Unlike previous sections, where we could lean on **Linear Guidance Law** when deflection angle passed 20 [°] limit, now we'll simulate a realized scenario. That is to say that the mechanical "Hard Boundary" of the servo unit will be pronounced as a **Saturation Block** in the regular guidance loop. Given $V_c = 1250\ [\frac{m}{sec}]$, $\dot{\lambda}_0 = 0.018\ [\frac{rad}{sec}]$, and the following System's IC : $X_1(0) = 0$, $X_2(0) = \dot{\lambda}_0 V_c t_F$. Where $X_2(0) = 0.018 \cdot 1250 \cdot 6 = 135\ [\frac{m}{sec}]$.

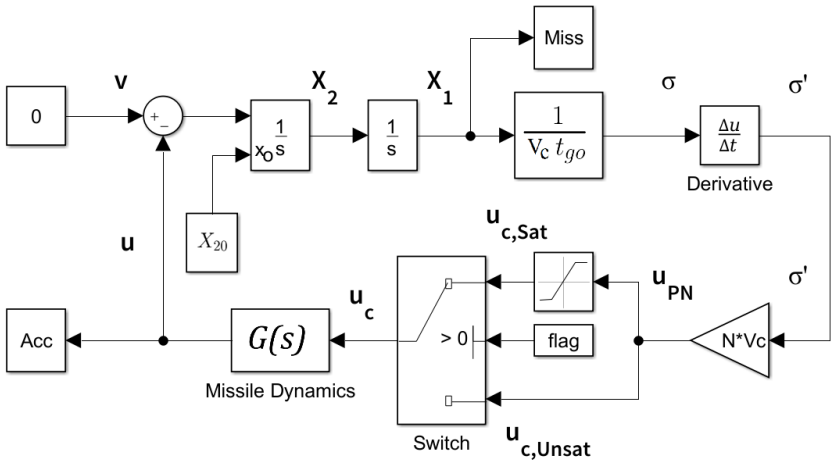

Figure 33: Regular guidance loop with switch node for both scenarios of Non/Saturated.

Let us look at the missile's required acceleration to satisfy capture :

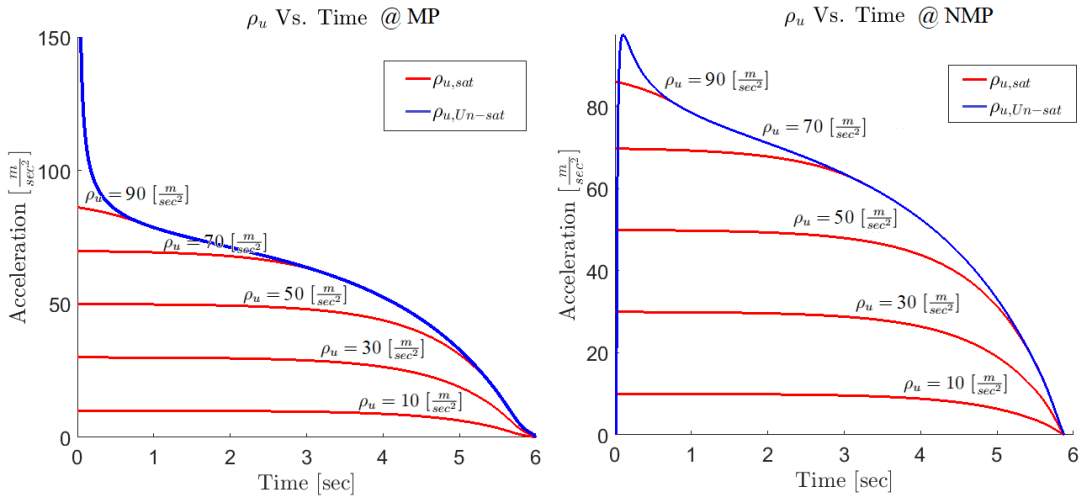

Figure 34: Saturated set of ρ_u under N' = 2.

Sanity check : when $N' = 2$ interceptor will be able to "snap out" of the saturation boundary, and follow the **Unsaturated** ρ_u towards t_f. One can see the typical difference between configurations, where NMP is once again exhibits poorer performances and lower boundaries.

Let's check the system's response under a **regular** set-up of $N' = 3$ for both configurations.
Note : After getting identical results for both MP and NMP, I combined graphs :

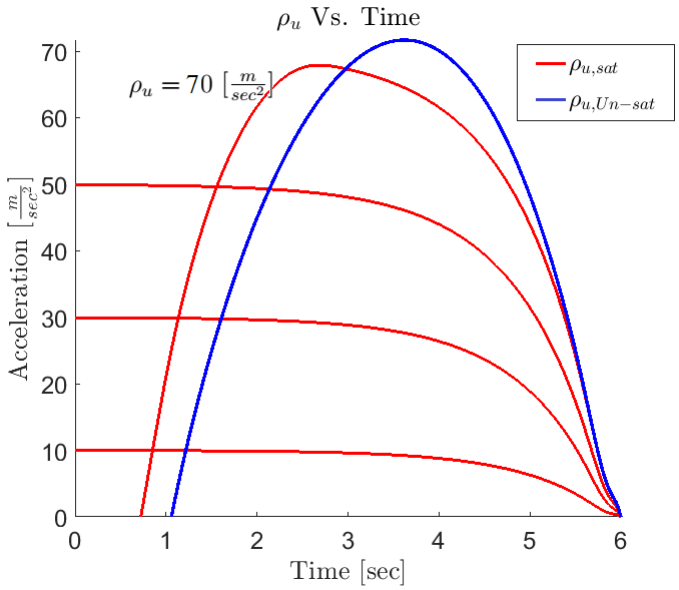

Figure 35: Accelerations obtained by set of Saturated ρ_u under N'=3 **(MP, NMP)**

From the course book, Saturation will take place once : $\rho_{u,cr} \geq \frac{N' X_{20}}{t_F} \rightarrow \rho_{u,cr} \geq 67.5\ [\frac{m}{sec^2}]$. As shown, smaller accelerations $\rho_u \leq 67.5\ [\frac{m}{sec^2}]$ are are forced to act so from t_0 to t_f. When $\rho_u \geq 67.5\ [\frac{m}{sec^2}]$ the accelerations get close to the **Unsaturated** graph, until convergence.

Let us now look at the obtained miss distances as a function of the missile's saturated ρ_u :

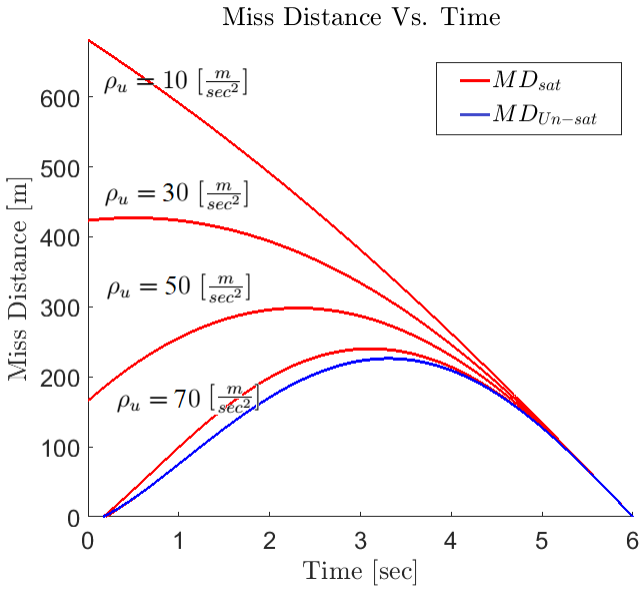

Figure 36: MD obtained by set of Saturated ρ_u under N'=3 **(MP, NMP)**

When the acceleration ratio between both sides is small $\mu = \frac{\rho_v}{\rho_v} \simeq 1$, the MD rises sharply meaning not any close capture. But when $\mu \downarrow$ the same phenomenon as before, goes here as well. As ρ_u gets closer to $\rho_{u,cr}$, the MD behaves like the unsaturated ρ_u, and slowly converges with him (Blue Line). That manner pronounce the **Non Linear** effect we've implemented in the system, once we broke **Linearity** Assumption.

7 Linear Optimal Guidance

7.1 Analytical Solution

In this section we are requested to find the navigation constant analytically, and look up for any sensitivity to the different parameters. Let us first define the following cost function :

$$J = |\mathbf{d}x(t_f)|^2 + \int_0^{t_f} \mathbf{k}u_c^2 dt$$

Where $\mathbf{d} = [1\ 0\ 0]$ ensures first elements, and $\mathbf{k}$ is the *penalty* on the control effort.

First we'll transform the problem into a Zero-Effort-Miss variable :

$y = \mathbf{d}\Phi(t_f, t)\mathbf{x} = x_1 + t_{go}x_2 - \mathcal{L}^{-1}\{c_M(sI - A_M)^{-1}/s^2\}\mathbf{z} = t_{go}^2\big[V_c\dot{\sigma} - \frac{1}{t_{go}^2}\mathcal{L}^{-1}\{c_M(sI - A_M)^{-1}/s^2\}\mathbf{z}\big]$

Transition Matrix : $\Phi = e^{At_{go}} = \mathcal{L}^{-1}\{c_M(sI - A_M)^{-1},$ and in the brackets :

$$(s\mathbf{I} - \mathbf{A})^{-1} = \begin{bmatrix} s\mathbf{I} & -\mathbf{I} & 0 \\ 0 & s\mathbf{I} & c_M \\ 0 & 0 & s\mathbf{I} - \mathbf{A}_M \end{bmatrix}^{-1} = \begin{bmatrix} \frac{1}{s}I & \frac{1}{s^2}I & -c_M(sI - A_M)^{-1}/s^2 \\ 0 & \frac{1}{s}I & c_M(sI - A_M)^{-1}/s \\ 0 & 0 & (sI - A_M)^{-1} \end{bmatrix}$$

Eventually we get the following form :

$\dot{y} = X(t_f, t)u_c$ and $X(t_f, t) = -\mathcal{L}^{-1}\{c_M(sI - A_M)^{-1}/s^2\}$

Which after using Riccati equation we get : $P = \frac{k}{k + \int_0^{tgo} X^2(\xi)d\xi}$

And the optimal guidance law becomes : $u_c^* = -k^{-1}XPy$

Substitute P, we get : $u_c^* = \frac{-X(t_{go})}{k + \int_0^{tgo} X^2(t_{go})dt_{go}} \cdot y$

Expressing the navigation constant : $N^*(t_{go}) = \frac{-X(t_{go})t_{go}^2}{k + \int_0^{tgo} X^2(\xi)d\xi}$

where $X(t_{go}) = -\mathcal{L}^{-1}\{G_M(s)/s^2\}$, and the autopilot dynamics :

$$G_M(s) = \frac{Ks^2 + KM_\delta}{\tau s^3 + (1+K)s^2 + k_{\dot{v}}M_\delta s + KM_\delta}$$

7.2 Practical Solution

Let us use the following algorithm that satisfies the N^* equation from above. **Note** that here, **k** is the **penalty** upon the control effort and regardless to the controller's K gain.

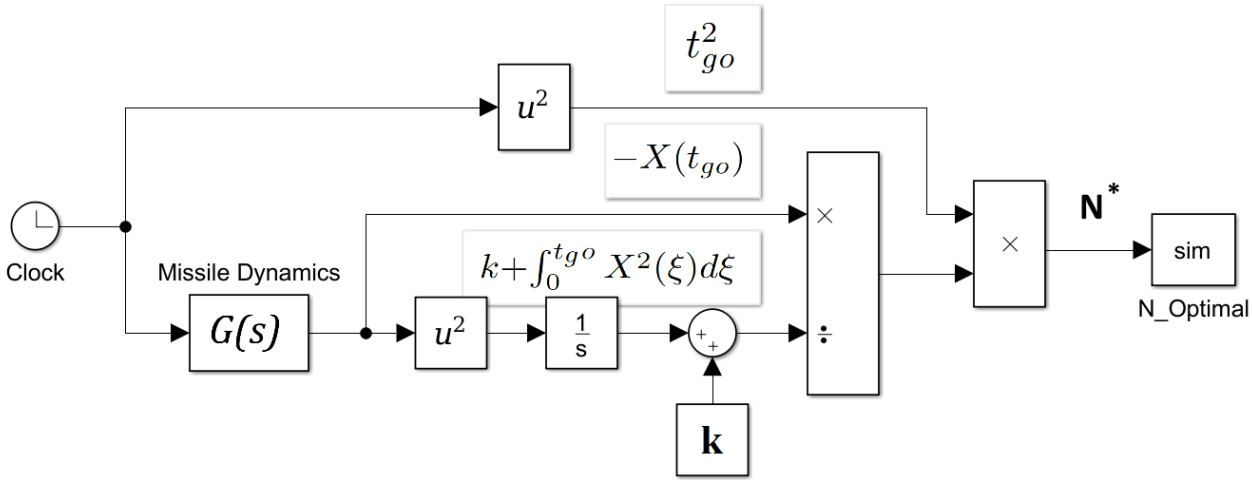

Figure 37: Simulink $\mathcal{L}^2$ Optimal Guidance Gain

Let us now simulate that diagram (above) and check the reciprocal between **k** and N^* :

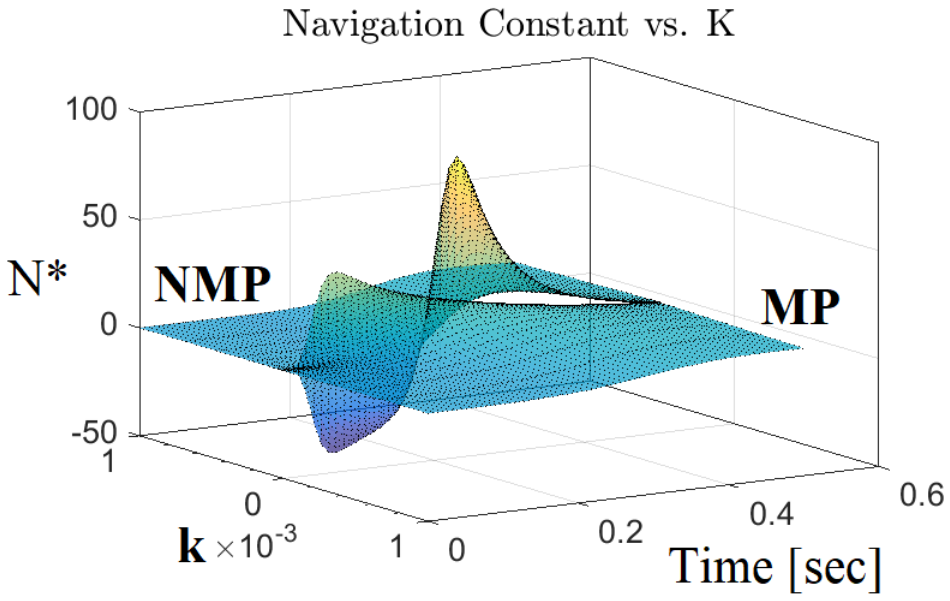

Figure 38: Navigation Constant vs. **k**

We can see from above (**Fig.** 38) the family responses of N^* where both configurations respond to the magnitude of **k**. Either here, the NMP exhibits *inverse response* of a negative N^* which is impossible. One can see that **only** in the vicinity of "0", i.e. very small **k** values, N^* rises sharply. Otherwise, we get N^* convergence towards small numbers around the "Lucky Number" $N' \simeq 3$, that is known to us from PN. **Conclusion :** if we don't want to pay **k** penalty, we must increase N^* gains respectively.

N* Sensitivity to Different Parameters

After checking sensitivity to several values of **k**, let us now fix $\mathbf{k} = 0.0001$ and present **only** the autopilot parameters that exhibited significant effect on N^*.

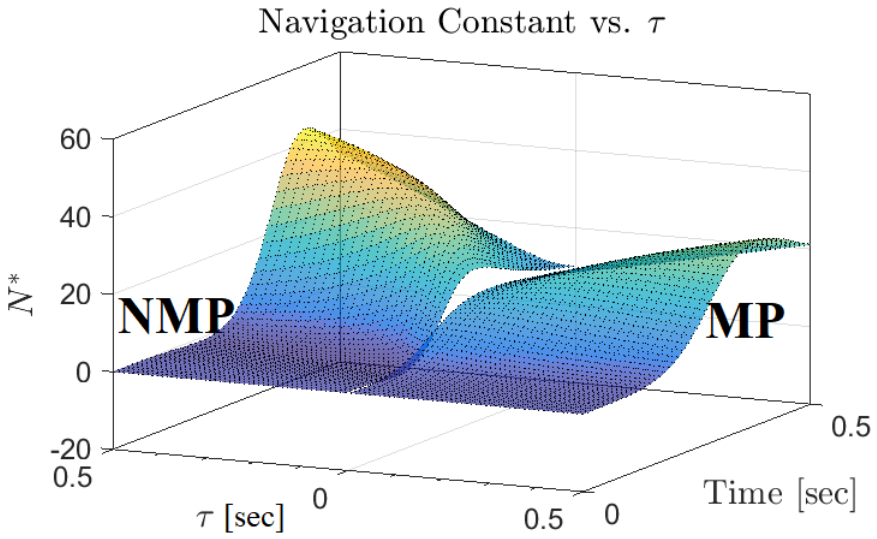

Figure 39: Navigation Constant vs. $\tau \in [0.005\ 0.5]$

We can see that while τ is rather small, we get a **relatively** small N^*. However, when τ increases, N^* rises steadily at both cases where in NMP it is more emphasized.

We shall now check the effective navigation response to the M_δ parameter :

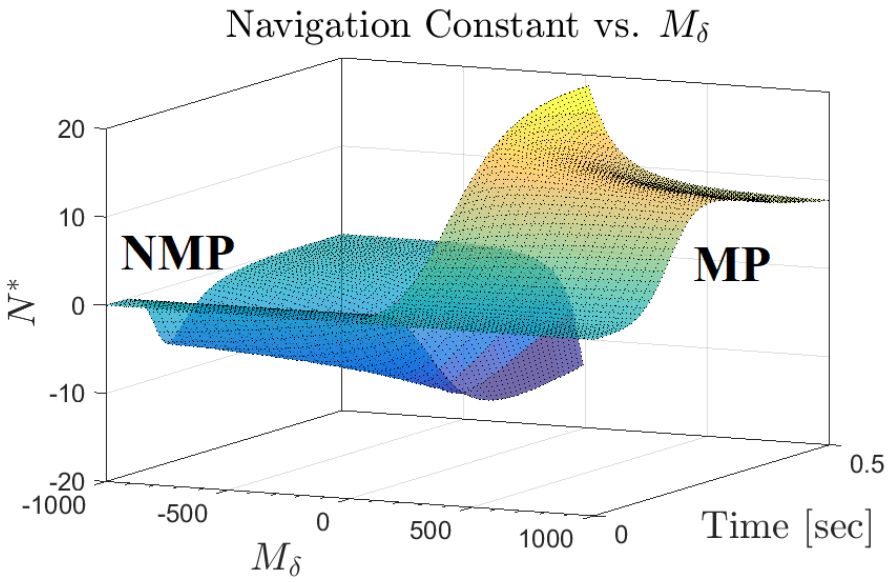

Figure 40: Navigation Constant vs. $M_\delta \in [10\ 1{,}000]$

We see the N^* response to M_δ at both configurations. Almost symmetrically, both respond sharply at low M_δ values. But when M_δ increased into reasonable values, N^* converges into more familiar low values. As for the inverse response between MP and NMP, it can be easily explained by the **sgn** of the u^* that exits the autopilot.

$-fin-$